CRACKING PRESSURE CONTROL OF PARYLENE CHECKVALVE USING SLANTED TENSILE TETHERS

Jeffrey Chun-Hui Lin, Feiqiao Yu, Yu-Chong Tai
California Institute of Technology, Pasadena, CA, U.S.A.

ABSTRACT

MEMS check valves with fixed cracking pressures are important in micro-fluidic applications where the pressure, flow directions and flow rates all need to be carefully controlled. This work presents a new surface-micromachined parylene check valve that uses residual thermal stress in the parylene to control its cracking pressure. The new check valve uses slanted tethers to allow the parylene tensile stress to apply a net downward force on the valving seat against the orifice. The angle of the slanted tethers is made using a gray-scale mask to create a sloped sacrificial photoresist with the following tether parylene deposition. The resulted check valves have both the cracking pressures and flow profiles agreeable well with our theoretical analysis.

INTRODUCTION

MEMS check valves are important components for microfluidic systems for the control of flow direction, flow rate and even pressure distribution. To implement controlable cracking pressures to normally-closed (NC) check valves, many different types of pre-stress technique have been utilized, such as cantilever type, diaphragm type, and bivalvular type, etc [1]. The mechanism of such NC check valves is to use deformation of covering materials, which are chosen and geometrically designed according to the requirements of applications. If high cracking pressure is necessary, materials having large Young's modulus are used to provide the required pre-stressed force.

We had reported several MEMS check valves using parylene C as the structure material. These parylene check valves had pre-stressed parylene membrane to the silicon surface using vacuum sealing and surface-to-surface stiction [2-4]. However, these approaches required complicated processing. In the case of vacuum-collapsed sealing check valve, the cracking pressure might drift with time because of gas permeation into the vacuum cavity. In the case of stiction-prestressed check valve also needed epoxied anchor to improve its reliability. Here, we present a much improved and reliable new approach of using pre-stressed slanted tethers to provide controllable cracking pressures. The valve schematic is shown in Fig.1. The check valve is thermally annealed at predetermined temperature after the sacrificial photoresist is released and quenched down afterwards. Since the residual tensile stress of the thermally annealed parylene C can be as high as 34 MPa at 250°C [5], this approach allows the parylene tethers to provide a high downward force while it does not require any post-fabrication fixation.

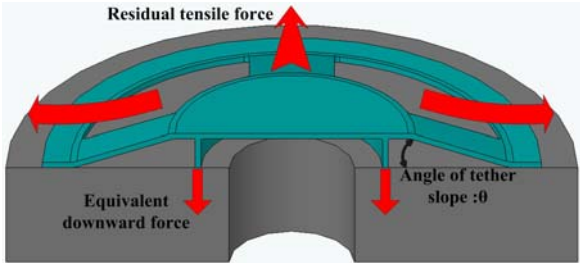

Figure 1: Schematic of cracking-pressure controlled parylene check valve using the residual tensile stress in parylene after thermal annealing.

CHECK VALVE DESIGN

In order to utilize the residual tensile stress in parylene after thermal annealing, we need to make parylene tethers slanted with an angle. After the check valves are processed with sacrificial photoresist etching, they are annealed at a desirable temperature and then quenched quickly to room temperature. Because the thermal expansion coefficient of parylene is much bigger than that of the silicon substrate, this process generates a tensile stress in the tethers. This residual tensile force then provides a net downward sealing force on the parylene valve seat against the silicon orifice. The final cracking pressure can be mathematically represented as

$$P_c = \frac{t \times w \times n \times \sigma_t \times \cos\theta \times \sin\theta}{\pi \times r^2}, \qquad (1)$$

where P_c is the cracking pressure of the valve; t is the thickness of the parylene; w is the width of the tethers; n is the number of the tethers; σ_t is the residual stress of thermally annealed parylene; θ is the angle of the tether slope; and r is the radius of the valving plate. It is shown that the cracking pressure can be controlled by many parameters such as the tethers geometry, parylene thickness, tethers' slope angle, and the annealing temperature. With the thermally annealing residual stress at 250°C as 34MPa, the cracking pressure of this check valve can be achieved as high as several psi even for a small check valve.

978-1-4244-5764-9/10/$26.00 ©2010 IEEE

SLOPED PHOTORESIST

The gray-scale photomask technique [6] is used in our fabrication process to make sloped sacrificial photoresist. Such a typical mask is shown in Fig.2. To make photoresist partially exposed, an array of small dark squares with pitch, p, smaller than the diffraction limit of the UV exposure system, p_c, are designed onto the photomask. Dark squares with pitch smaller than diffraction limit can actually make the first order diffraction light blocked by the numerical aperture of the exposure system, making the light transmittance of the photomask proportional to the coverage area of these dark squares [7]. The maximum square pitch size can be expressed as

$$p \le p_c = \frac{1}{1+\sigma} \times \frac{\lambda}{NA}, \qquad (2)$$

where σ is the coherence factor of the optical system, λ is the UV wavelength and NA is the numerical aperture of the exposure system [8]. According to the specification of our exposure stepper, the diffraction limit is about 1 μm. With the 10:1 optical image reduction, we can have dark squares >10 μm on our photomask. Therefore, it is relatively low-cost to perform the gray-mask lithography [9]. In the transmittance design, "pulse width modulation" approach is used, in which a constant square pitch with various dark square sizes is shown in Fig.2.

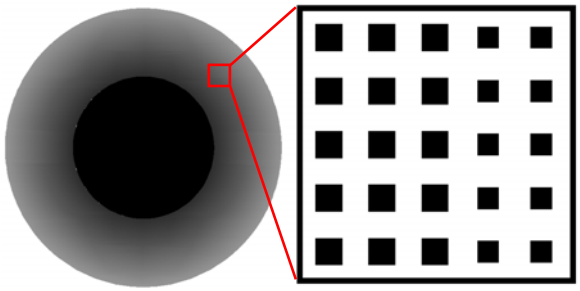

Figure 2: A closer view of designed gray photomask for the creation of sloped photoresist. The right pattern shows the part of pixel structure of the ring.

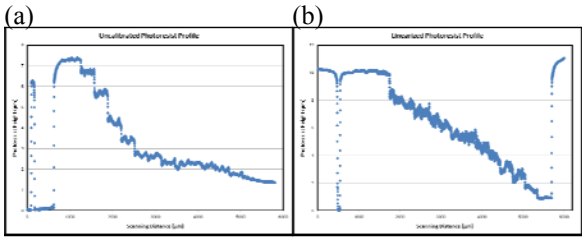

Figure 3: Gray-scale photoresist profile: (a) before linearization, and (b) after linearization.

Nevertheless, most photoresists have nonlinear response to UV light exposure so a gray-scale photomask pattern with linear transmittance distribution will not give us a linear photoresist profile, as shown in Fig.3a. A mathematical model is adopted here to characterize and linearize our final photoresist profile [10]. In the model, the original total percentage of unexposed photoresist is normalized as 1, and the percentage of exposed photoresist is denoted as E(t), which is generated after exposure to UV light within a period of time, t. It is further assumed that the changing rate of exposed photoresist, $\dot{E}(t)$, is proportional to the remaining unexposed photoresist, $1-E(t)$, and the exposed light intensity I_0T, where I_0 is the stepper light intensity and T is the transmittance of the photomasks. Therefore, the overall exposure system can be represented as an ordinary differential equation with the initial condition as follows,

$$E(0) = 0, \qquad (3)$$

and

$$\dot{E}(t) = \alpha(1-E(t))I_0T, \qquad (4)$$

where α is the proportional constant. The constant is an optical property of the photoresist's sensitivity to UV light. The solution of equation (3) and (4) can be obtained as

$$E(t) = 1-\exp(-\alpha I_0 T t). \qquad (5)$$

Therefore, to have a linear distribution of exposed photoresist, E(t), we can use Eq.(5) to design the corresponding transmittance distribution on photomask. Fig.2b then shows the scanning result of the characterized and then linearized photoresist profile.

In Fig.2b, the gray-scale photomask is composed of 16 levels with increasing transmittance from left to the right of the sloping area with each level translating into a photoresist height proportional to $\exp(-\alpha I_0 t)$. In order to create a true linear slope, a test photoresist strip was first fabricated for characterization. Then, the transmittance of each ring is adjusted according to the resulted photoresist height from the test strip. It was shown in literature that larger $\alpha I_0 t$ produces more reliable results [10]. In our case, I_0 is measured as 200-250 mw/cm^2 in the stepper, which is one order of magnitude higher than the published literature. With *t* taken as 4 seconds, our exposure energy is within the right regime suggested in the literature.

FABRICATION

Fabrication procedures are outlined in Fig.4. The process started with thermally growing silicon dioxide on both sides of double-side-polished wafers. After a back side oxide patterning, DRIE was used to etch the backside holes, 90µm in diameter, until a thin silicon membrane of 50µm was left. XeF_2 was then used on the front side to roughen the silicon surface around the periphery of the valve seat to create robust anchors. A 10µm photoresist AZ4620 was then coated on the front side and patterned using a gray-scale mask. A 2-step exposure technique with different exposure times was utilized to make the center sealing photoresist to have variable height. DRIE was then employed to etch through the backside trenches and holes after a 5µm parylene is coated and patterned. After sacrificial photoresist was stripped by acetone and IPA, a thermal annealing was performed, where different temperatures were used to create different residual stresses. SEM images of fabricated devices before and after photoresist stripping are shown in Fig.5. Figs.5a&b illustrate the successful creation of the slanted sacrificial photoresist profile and Fig.5c&d show the resulted linearly slanted parylene tethers after removing the photoresist.

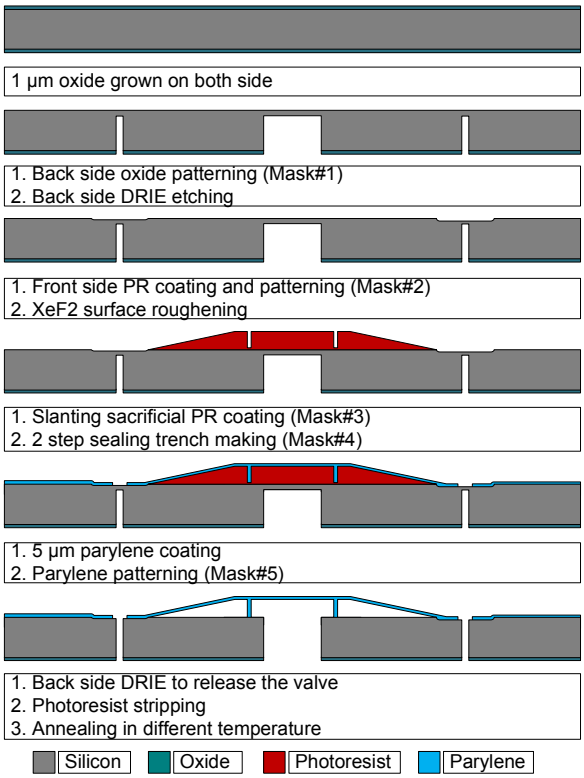

Figure 4: Fabrication procedures.

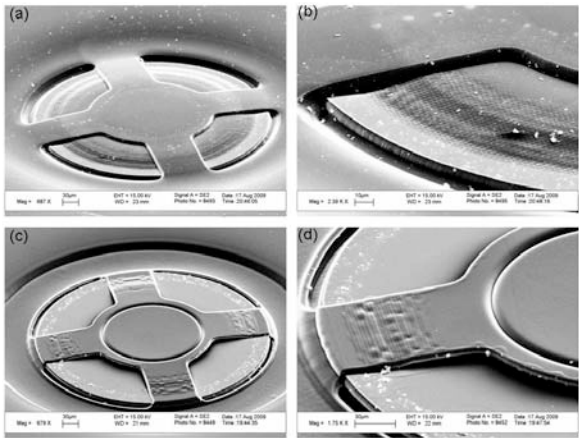

Figure 5: SEM pictures of fabricated valves: (a) valves before photoresist removal; (b) a closer view of a tether, (c) valves after photoresist removal; (d) a closer view of a tether.

DEVICE TESTING AND DISCUSSION

After photoresist removal, the slanted-tether valves were tested using the setup shown in Fig.6. Pressure was applied to the valve through the backside holes and flow rate was recorded. For valves annealed at 100°C, valves of 3 different tether widths were tested (50µm, 70µm, 100µm). The cracking pressures were measured to be 0.3psi, 1.5psi, and 2.9psi respectively as shown in Fig.7a. The valve's cracking pressure increases as the tethers widen, which is as expected because increased width means increased prestressed force. The flow profiles of two 50µm-wide-tether valves annealed differently at 100°C and 140°C were also compared, as shown in Fig.7b. The cracking pressures were 0.3 psi and 1.3 psi respectively. The increased cracking pressure is due to the increased thermal residual stress of parylene when the annealing temperature was increased. To summarize, experimental cracking pressures of valve with different tether widths and annealing temperature were consistent with the valve designs. However, experimental data also showed that the cracking pressure could be different from the theoretical value when annealed at too high a temperature. This is believed to be caused by parylene oxidation since the parylene was baked in the air.

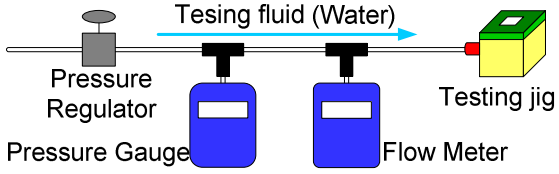

Figure 6: Testing setup.

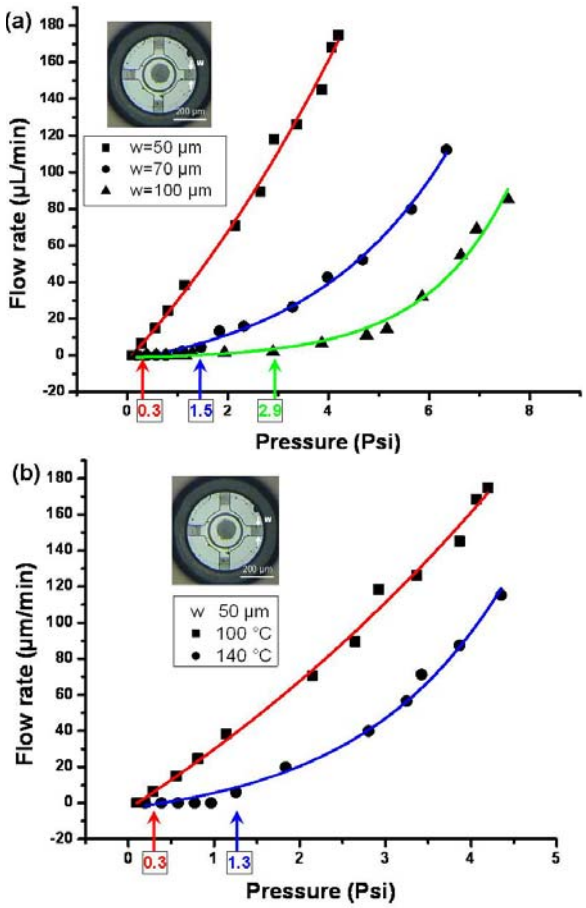

Figure 7: Cracking pressure results of (a) different tether widths but the same annealing at 100°C, and (b) same tether width (50 µm) but different annealing temperatures.

CONCLUSION

A new MEMS parylene check valve pre-stressed by the residual thermal stress induced after parylene annealing was demonstrated. This was achieved by using slanted tethers that provide a net downward force onto the parylene valve seat against the orifice. To create the slanted tethers, a linearly sloped sacrificial photoresist was created using a gray-scale photomask technique. As expected, the fabricated check valves did show high cracking pressures and low flow rates. Moreover, the resulted cracking pressures and flow profiles also agreed well with the theoretical analysis.

ACKNOWLEGDEMENTS

The authors would like to thank Mr. Trevor Roper for his valuable fabrication assistance.

REFERENCES

[1] M. Koch, A. Evans and A. Brunnschweiler, *Microfluidic Technology and Applications*, Philadelphia, Research Studies Press Ltd., 2000

[2] P.-J. Chen, D. C. Rodger, E. M. Meng, M. S. Humayun and Y.-C. Tai, "Surface-Micromachined Parylene Dual Valves for On-Chip Unpowered Microflow Regulation," *J. Micoelectromech. Syst.*, vol. 16, pp. 223–231, 2007.

[3] J. C.-H. Lin, P.-J. Chen, S. Saati, R. Varma, M. Humayun and Y.-C. Tai, "Implantable Microvalve-Packaged Glaucoma Drainage Tube," in *Tech. Digest 13th Solid State Sens., Actuators, and Microsyst. Workshop*, Hilton Head, SC, Jun. 1-5, 2008, pp. 146–149.

[4] J. C.-H. Lin, P.-J. Chen, B. Yu, M. Humayun and Y.-C. Tai, "Minimally Invasive Parylene Dual-valved Flow Drainage Shunt for Glaucoma Implant," in *Tech. Digest 22nd IEEE International Conference on Microelectromechanical Systems (MEMS 2009)*, Sorrento, Italy, Jan. 25-29, 2009, pp.196-199.

[5] S Dabral, J. Van Etten, X. Zhang, C. Apblett, G.-R. Yang, P. Ficalora, and J. F. McDonald, "Stress in Thermally Annealed Parylene Films," *J. Electron. Mater.*, Vol. 21, No. 10, pp. 989-994, 1992.

[6] Y. Oppliger, P. Sizt, J.M. Stauffer, J.M. Mayor, P. Regnault and G. Voirin, "One-step 3D Shaping Using a Gray-Tone Mask for Optical and Microelectronic Applications," *Microelectronic Engineering*, 23, pp. 449-454, 1994.

[7] C. M. Waits, A. Modafe and Reza Ghodssi, "Investigation of Gray-scale Technology for Large Area 3D Silicon MEMS Structures," J. Micromech. Microeng. 13 pp. 170-177, 2003.

[8] B. Wagner, H.J. Quenzer, W. Henke, W. Hoppe and W. Pilz, "Microfabrication of Complex surface Topographies Using Grey-tone Lithography," Sensors and Actuators A, 46-47, pp. 89-94, 1995.

[9] T. J. Suleski and D. C. O'Shea, "Gray-scale Masks for Diffractive-optics Fabrication: I. Commercial Slide Imagers," *Appl. Opt.*, Vol. 34, No. 32, pp. 7507-7517, 1995.

[10] M. LeCompte, X. Gao and D. W. Prather, "Photoresist Characterization and Linearization Procedure for The Gray-Scale Fabrication of Diffractive Optical Elements," *Appl. Opt.*, Vol. 40, No. 32, pp.5921-5927, 2001.